

RESEARCH NOTE

Open Access



# Unique microglia expression profile in developing white matter

Ori Staszewski and Nora Hagemeyer\*

## Abstract

**Objective:** Recently we demonstrated that amoeboid microglia in white matter regions are essential for proper oligodendrocyte homeostasis and myelinogenesis in the first postnatal week. Amoeboid microglia in the mouse corpus callosum change their activation profile within few days after postnatal day (P)7 with microglia of the cerebellum showing similar features. Here we expanded our previous transcriptional analysis and performed detailed bulk RNA sequencing of microglia from corpus callosum, cortex and cerebellum at P7, P10 and P42. The goal of this study was to identify a specific gene profile for both, white matter and grey matter microglia during development.

**Results:** Microglia in white matter regions display unique characteristics in the first postnatal week of murine life. In both the corpus callosum and cerebellum microglia show amoeboid morphology and a similar transcription profile during development including high expression of genes related to priming of microglia, phagocytosis and migration at P7; characteristics which are already lost at P10. Together these data verify our previous transcriptional data obtained by microarray analysis and enable a more complete view into white matter and grey matter microglia at different developmental stages.

**Keywords:** Amoeboid microglia, RNA sequencing, White matter, Grey matter

## Introduction

Microglia are the resident myeloid cells in the brain parenchyma with diverse functions during homeostasis and disease [1]. The accumulation of activated microglia with an amoeboid morphology along the ventricles and white matter regions within the first postnatal week was described as early as 1932 [2, 3]. This phenomenon was not restricted to rodents; in 1939 Kershman coined the term “fountain of microglia” for hot spots of activated microglia during human embryogenesis [4]. Many decades later this phenomena was confirmed by several studies [5–10]. Their function, however, has remained unknown. Recently we identified an essential role for amoeboid microglia in murine white matter regions for oligodendrocyte homeostasis and myelinogenesis during the first postnatal week [11], an observation which was replicated shortly after [12]. On the transcriptional

level, microarray based analysis showed that microglia of the corpus callosum (CC) at postnatal day (P)7 are highly activated compared to cortical microglia. As we observed that the amoeboid phenotype rapidly changed within a few days after P7 and cerebellar microglia appeared to display very similar characteristics to callosal microglia, we proceeded here to analyze microglia during development in a more detailed way, by assessing P7, P10 and adult (P42) microglia from the CC, cortex (Cx) and cerebellum (Cb) with bulk RNA sequencing. Our data identify that the transcriptional profile of microglia in the CC and Cb at P7 and P10 is driven largely by age and much less by the specific brain region assayed and cortical microglia show a transcriptional profile different from white matter microglia. Finally, at P42 microglia from all brain regions appeared to share a common transcriptional pattern. These data suggest that early during postnatal development white matter microglia in all brain regions possess a unique transcriptional profile compared with grey matter that is lost during maturation.

\*Correspondence: nora.hagemeyer@uniklinik-freiburg.de  
Institute of Neuropathology, Medical Faculty, University of Freiburg,  
Breisacher Str. 64, 79106 Freiburg, Germany



## Main text

### Materials and methods

#### Mice

*Cx3cr1<sup>GFP/WT</sup>* and wildtype (C57BL/6 J) mice were bred in-house under pathogen-free conditions. All animal experiments were approved by the Regierungspräsidium Freiburg, Germany, Section: Landwirtschaft, Ländlicher Raum, Veterinär- und Lebensmittelwesen. Application no. G17/55 and X-16/04.

#### Cell sorting and histology

Tissue samples were prepared as described before [11, 13]. Briefly, mice were lethally anesthetized and perfused. Brain tissue was fixed in 4% PFA for immunohistochemistry or brain regions were separated and homogenized for cell sorting.

Cell sorting was done on a MoFlo Astrios (Beckman Coulter, Krefeld, Germany). Live/Dead stain: Fixable Viability Dye eFluor<sup>®</sup>506 (eBioscience, San Diego, USA). Fc block: Fc-receptor blocking antibody CD16/CD32 (clone:2.4G2, BD Bioscience, Heidelberg, Germany). Antibodies used: anti-CD45 (clone:30-F11, eBioscience, San Diego, USA), anti-CD11b (clone:M1/70, eBioscience, San Diego, USA), anti-Gr1 (clone:RB6-8C5, Biolegend, Fell, Germany).

For immunofluorescence staining tissues were treated as described before [11]. Briefly, mouse brains were fixed overnight, dehydrated and embedded in Tissue-Tek<sup>®</sup>O.C.T.TM Compound (Sakura Finetek Europ B.V., Netherlands). 12 µm cryosections were stained. Primary antibodies used: IBA-1 (1:500, Cat. No.: NB100-1028, Novus Biologicals, Wiesbaden, Germany), SPP1 (1:200, Cat. No.: ab8448, abcam, Berlin, Germany), CLEC7A (1:30, Cat. No.: mabg-mdect, InvivoGen, Toulouse, France) and CD206 (1:100, Cat. No.: MCA2235, Bio-Rad, Munich, Germany). Secondary antibodies used: Alexa Fluor 555, Alexa Fluor 568, Alexa Fluor 488, Alexa Fluor 647 1:500 (Life technologies, Darmstadt, Germany). Nuclei counterstaining: 4,6-diamidino-2-phenylindole (DAPI, 1:10,000, Cat. No.: 236276, Boehringer, Mannheim, Germany). Imaging was performed on the BZ-9000 Bioevo microscope (Keyence, Neu-Isenburg, Germany). N = 3–4/timepoint. Quantification of microglia (Fig. 1c) was performed on three parasagittal brain sections (every 10th section starting at the level of the rostral migratory stream) per animal (N = 3 mice).

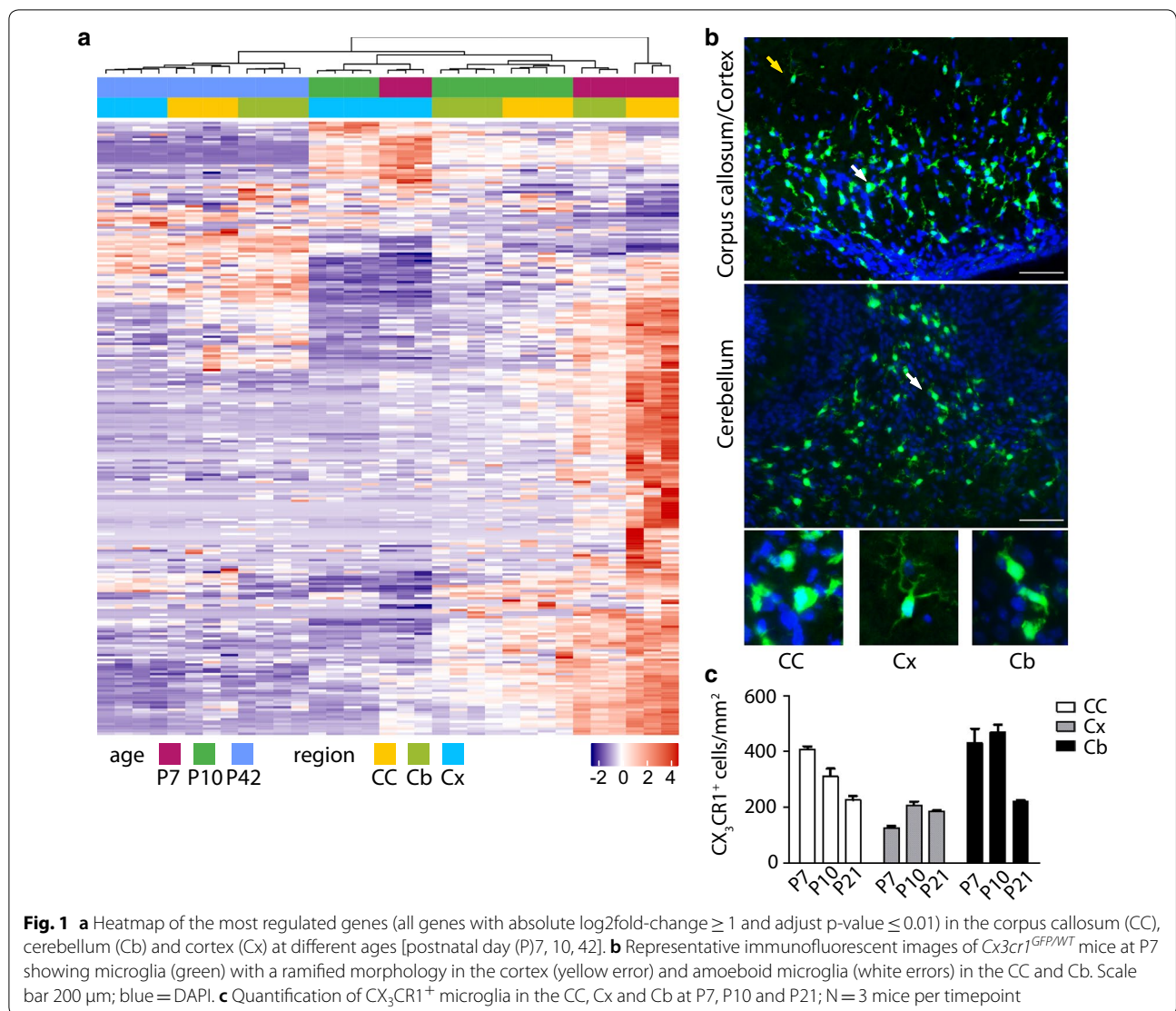
#### RNA sequencing

FACS-sorted microglia were processed at the Genomics Core Facility “KFB-Center of Excellence for Fluorescent Bioanalytics” (University of Regensburg, Regensburg, Germany; <http://www.kfb-regensburg.de>). Library preparation and RNA sequencing was performed as described

before [13]. Quality control of Fastq Files was done using FastQC [14]. Using the Star aligner (version 2.5.2b), reads were mapped to the GRCm38 mouse genome [15]. Read counts were acquired by the featureCounts (version 1.6.2) package with essentially standard settings. Specifically counts were combined at the gene level, multimapping and multi overlapping counts were discarded and reads were required to overlap by at least 1 base with an annotated feature. Differential gene expression analysis was done by the limma/voom (version 3.38) pipeline in R following the limma vignette [16–18]. Specifically genes with zero reads were discarded. Following counts were summarized for each gene over all samples and the lower third of genes were removed (averaging to about 1.5 counts per sample). After prefiltering the limma/voom pipeline was followed as described the vignette. Heatmaps were created using the ComplexHeatmaps R package [19]. Pathway Analysis was conducted using Ingenuity Pathway Analysis (IPA, Qiagen). For IPA analysis all genes with an adjust p-value of <0.01 were retained and IPA analysis was performed with standard settings except that only experimentally observed interactions in mouse datasets were queried.

#### Results

To investigate the expression profile of microglia during development in white and grey matter regions, we performed bulk RNA sequencing of fluorescent activated cell sorted (FACS) microglia (CD45<sup>+</sup>, CD11b<sup>+</sup>, Gr<sup>-</sup>) of the CC, Cx and Cb at postnatal day P7, P10 and P42. By analyzing the gene expression of microglia at these different ages and brain regions it became clear, that microglia of the CC and Cb display a similar expression profile. In these brain regions, the developmental stage had a higher impact on gene expression compared to brain region itself (Fig. 1a). In contrast, cortical microglia at P7 and P10 clustered separately from CC and Cb microglia at P7 and P10. This suggests that, in this instance, the brain region itself had higher impact on the gene profile of cortical microglia than did age. Finally, at P42, microglia of all brain regions investigated were quantitatively similar at the gene expression level. Next, using *Cx3cr1<sup>GFP/WT</sup>* mice to assess microglia morphology using immunofluorescent analysis, we observed that microglia of the CC and Cb at P7 had an amoeboid shape, indicative of a high activation state of these cells (Fig. 1b white arrow). In contrast, cortical microglia had a ramified -not activated-morphology (Fig. 1b yellow arrow). Moreover, cell dynamics during development were very similar in the CC and Cb showing higher cell numbers at P7 and P10 compared to cortical microglia which decreased until P21 (Fig. 1c). Cortical microglia numbers increased up to P10 and showed a milder subsequent decline. Together

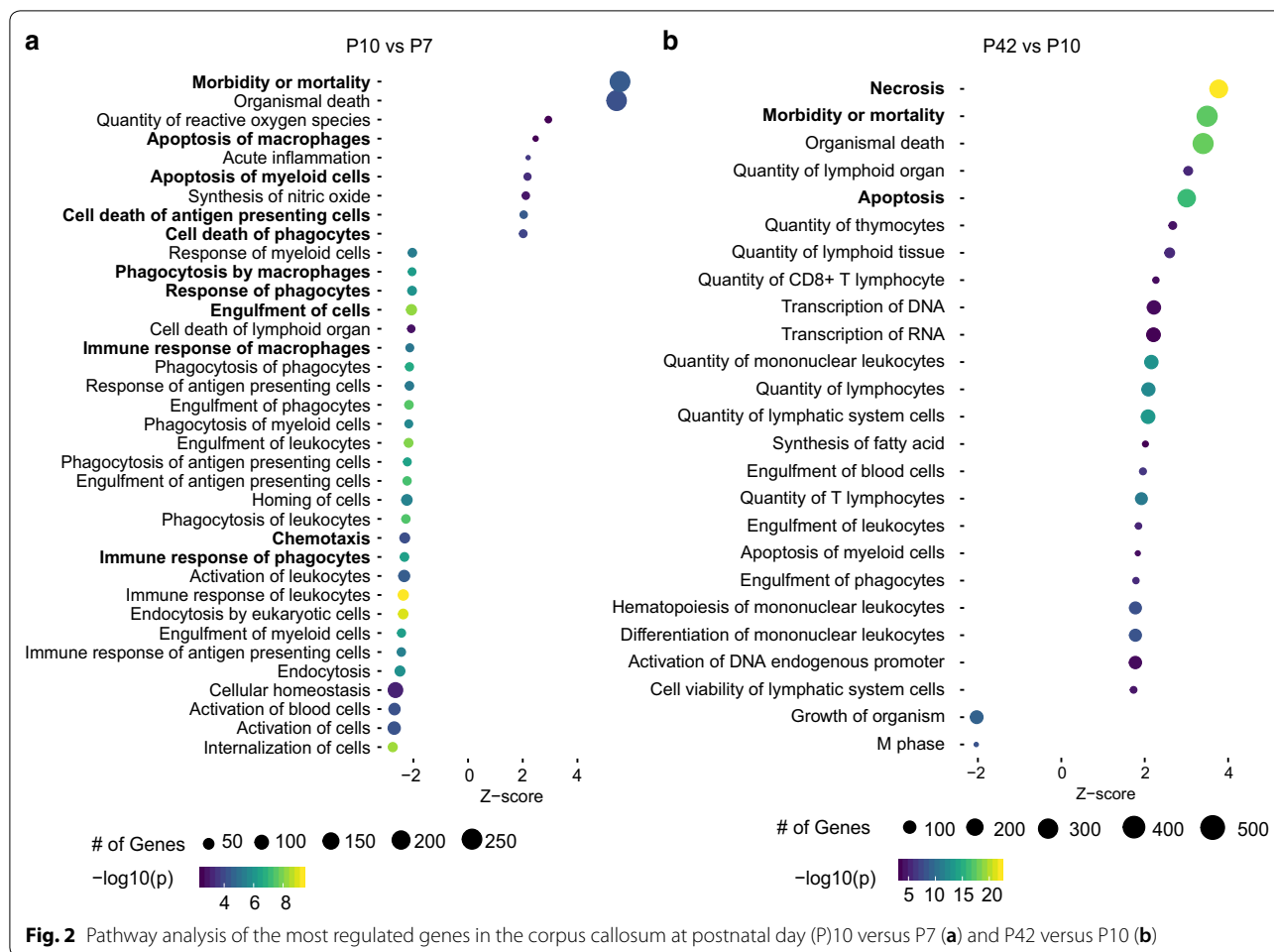


these data indicate that developmental transcriptional profile, morphological phenotype, and cell dynamics are similar between microglia of the CC and Cb and different from cortical microglia.

To more closely assess differences in gene expression over time, we performed pathway analyses, which demonstrated a higher expression of genes related to apoptosis at P10 compared to P7 in the CC, whereas at P7, genes related to phagocytosis and chemotaxis were highly upregulated compared to P10 (Fig. 2a). Interestingly, with further maturation (comparison of microglia at P42 to P10) mainly genes related to apoptosis and necrosis were highly expressed in the CC (Fig. 2b). A similar profile could be seen for microglia in the Cb and Cx related to apoptosis (data not shown), whereas genes related to phagocytosis (e.g. *Gsn*, *Cd36*, *Abca1*, *Grk6* and *Scarb1*)

were not expressed as highly as in the CC and were not as strongly altered over time (Fig. 3a).

Finally, we carried out hierarchical clustering of known priming genes as *Axl*, *Mrc1*, *Gas7*, *Clec7a*, *Igf1*, *Spp1*, *Anxa5*, *Gpnmb*, *Itgax*, *Lgals3*, *Cd36* and *F13a1*, which suggested that these genes are highly upregulated in P7 CC microglia. In contrast, Cb microglia at P7 showed a somewhat lower upregulation of these genes, while no expression was observed in cortical microglia (Fig. 3b). At P10, upregulation of these genes was no longer observed in any of the three regions assessed. Finally, in agreement with the transcriptional assessment we observed clear expression of SPP1, CLEC7A and CD206 (*Mrc1*) in IBA-1<sup>+</sup> microglia at P7 in the CC by immunohistochemistry (Fig. 3c, d)



which was not detectable in the CC at P10 (Fig. 3c, d). Interestingly, in the Cb CLEC7A and CD206 were not expressed in white matter microglia at any timepoint, however single positive SPP1<sup>+</sup> microglia or patches of SPP1<sup>+</sup> microglia could only be found in the central area of the white matter at P7 (Fig. 3c right (arrow), Additional file 1: Figure S1b). No expression of SPP1, CLEC7A and CD206 could be found in microglia of the cortex at any timepoint (Fig. 3e left; Additional file 1: Figure S1a). These data, again, demonstrate similar phenotype of white matter microglia early in development and a strong transcriptional dynamic occurring over just a few days.

**Discussion**

Here we have demonstrated a detailed RNA sequencing analysis of murine microglia of white and grey matter regions over different developmental stages. This complements our previous data which identified specific properties of a microglia subpopulation which is only present in the developing CC and cerebral white

matter. First, we could demonstrate here that microglia of white matter regions, namely the CC and Cb, are closely related to each other at P7 and P10 compared to cortical grey matter microglia. Second, microglia in both CC and Cb undergo a change in their gene expression profile between P7 and P10, demonstrating rapid alterations specific to white matter microglia at these developmental stages. At P7, CC and Cb microglia display a distinct transcriptional profile, including genes related to phagocytosis and migration as well as priming of microglia described during aging and disease [20, 21]. Genes related to apoptosis and necrosis, instead, are highly expressed at P10, and further increased at P42. The unique phenotype of P7 CC microglia was further confirmed in assessment of SPP1, CLEC7A and CD206 protein immunoreactivity, which was uniquely present at this timepoint, while not present in the cortical microglia and only partly recapitulated (SPP1 expression) in microglia of the Cb. Third, in contrast to white matter microglia, gene transcription of cortical microglia was driven by the brain region itself and was therefore distinct



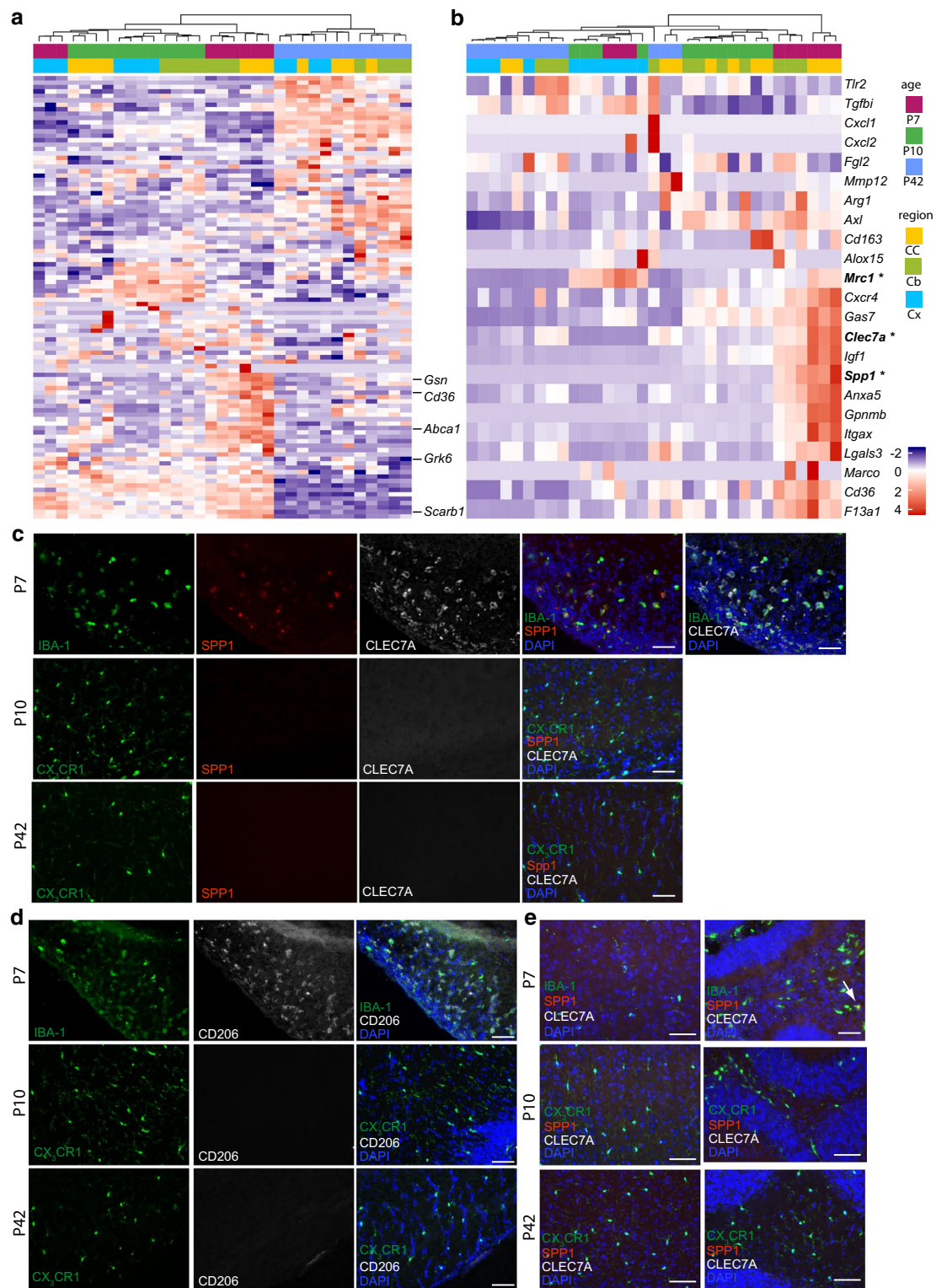


**Fig. 3** **a** Heatmap of regulated genes related to phagocytosis in the corpus callosum (CC), cerebellum (Cb) and cortex (Cx) at different ages [postnatal day (P)7, 10, 42]. **b** Heatmap of known priming genes in the CC, Cb and Cx at P7, P10 and P42. Asterisks highlighting genes confirmed on protein level; Representative immunofluorescence pictures of wildtype mice depicting SPP1 [red (**c**, **e**)], CLEC7a [white (**c**, **e**)] and CD206 [white (**d**)] expression in IBA-1<sup>+</sup> microglia (green) in the CC (**c**, **d**), Cx (**e** left) and Cb (**e** right) at P7, P10 and P42. Scale bar 50 μm; blue = DAPI; arrow indicating IBA-1<sup>+</sup>/SPP1<sup>+</sup> cell in Cb; N = 3–4 mice per timepoint

from white matter microglia. Fourth, gene expression of microglia was similar across regions in the adult brain. These results indicate that white matter microglia, perhaps by migration and phagocytosis, may play a special role in local tissue dynamics around P7, impacting oligodendrocyte homeostasis and myelination. This role is likely restricted to a brief window of time, after which cell numbers decline through apoptosis. As maturation continues into adulthood, resident microglial populations develop a common homeostatic role across white and grey matter regions. It will be of interest to understand the responsible molecular mechanisms and functional consequences in future studies.

## Limitations

- Transcriptional data are presented without functional analyses.
- Juvenile stages could have been included.

## Additional file

**Additional file 1: Figure S1.** Representative immunofluorescent images of wildtype or *Cx3cr1<sup>GFP/WT</sup>* mice presenting expression of SPP1 (red), CLEC7A (white) and CD206 (white) in IBA-1<sup>+</sup> or CX<sub>3</sub>CR1<sup>+</sup> microglia in the cortex (a) and cerebellum (b) at P7, P10 and P42. Scale bar 50 μm; blue = DAPI; arrow indicating IBA-1<sup>+</sup>/SPP1<sup>+</sup> cell in Cb; N = 3–4 mice per timepoint.

## Abbreviations

CC: corpus callosum; Cx: cortex; Cb: cerebellum; CNS: central nervous system; P: postnatal day; FACS: fluorescent activated cell sorting.

## Acknowledgements

We thank Prof. Marco Prinz for his support of this study as well as Jaclyn Wamsteeker Cusulin for critically reading and editing the manuscript.

## Authors' contributions

NH designed and conducted the experiments. OS analyzed the RNA sequencing data. NH and OS wrote the manuscript. Both authors read and approved the final manuscript.

## Funding

This work received no funding.

## Availability of data and materials

The main GEO accession number for RNAseq data: GSE132688

## Ethics approval and consent to participate

All animal experiments were approved by the Regierungspräsidium Freiburg, Germany, Section: Landwirtschaft, Ländlicher Raum, Veterinär- und Lebensmittelwesen. Application No. G17/55 and X-16/04.

## Consent for publication

Not applicable.

## Competing interests

The authors declare that they have no competing interests.

Received: 17 April 2019 Accepted: 26 June 2019  
Published online: 01 July 2019

## References

1. Prinz M, Erny D, Hagemeyer N. Ontogeny and homeostasis of CNS myeloid cells. *Nat Immunol*. 2017;18:385.
2. Rio-Hortega P. Microglia. *Cytol Cell Pathol Nerv Syst*. 1932;2:482–534.
3. Sierra A, de Castro F, del Río-Hortega J, Rafael Iglesias-Rozas J, Garrosa M, Kettenmann H. The "Big-Bang" for modern glial biology: translation and comments on Pío del Río-Hortega 1919 series of papers on microglia. *Glia*. 2016;64:1801–40.
4. Kershtan J. Genesis of microglia in the human brain. *Arch Neurol Psych*. 1939;41:24–50.
5. Chertoff M, Shrivastava K, Gonzalez B, Acarin L, Giménez-Llort L. Differential modulation of TREM2 protein during postnatal brain development in mice. *PLoS ONE*. 2013;8:e72083.
6. Hristova M, Cuthill D, Zbarsky V, Acosta-Saltos A, Wallace A, Blight K, et al. Activation and deactivation of periventricular white matter phagocytes during postnatal mouse development. *Glia*. 2010;58:11–28.
7. Dalmau I, Vela JM, González B, Finsen B, Castellano B. Dynamics of microglia in the developing rat brain. *J Comp Neurol*. 2003;458:144–57.
8. Ellison JA, de Vellis J. Amoeboid microglia expressing GD3 ganglioside are concentrated in regions of oligodendrogenesis during development of the rat corpus callosum. *Glia*. 1995;14:123–32.
9. Verney C, Monier A, Fallet-Bianco C, Gressens P. Early microglial colonization of the human forebrain and possible involvement in periventricular white-matter injury of preterm infants. *J Anat*. 2010;217:436–48.
10. Rezaie P, Male D. Colonisation of the developing human brain and spinal cord by microglia: a review. *Microsc Res Tech*. 1999;45:359–82.
11. Hagemeyer N, Hanft K-M, Akriditou M-A, Unger N, Park ES, Stanley ER, et al. Microglia contribute to normal myelinogenesis and to oligodendrocyte progenitor maintenance during adulthood. *Acta Neuropathol (Berl)*. 2017;134:441–58.
12. Włodarczyk A, Holtman IR, Krueger M, Yogev N, Bruttger J, Khoroshi R, et al. A novel microglial subset plays a key role in myelinogenesis in developing brain. *EMBO J*. 2017;36:3292.
13. Datta M, Staszewski O, Raschi E, Frosch M, Hagemeyer N, Tay TL, et al. Histone deacetylases 1 and 2 regulate microglia function during development, homeostasis, and neurodegeneration in a context-dependent manner. *Immunity*. 2018;48(5):514–529.e6.
14. Andrews S. FastQC: a quality control tool for high throughput sequence data. 2010. <http://www.bioinformatics.babraham.ac.uk/projects/fastqc>.
15. Dobin A, Davis CA, Schlesinger F, Drenkow J, Zaleski C, Jha S, et al. STAR: ultrafast universal RNA-seq aligner. *Bioinf Oxf Engl*. 2013;29:15–21.
16. Law CW, Chen Y, Shi W, Smyth GK. voom: precision weights unlock linear model analysis tools for RNA-seq read counts. *Genome Biol*. 2014;15:R29.
17. Ritchie ME, Phipson B, Wu D, Hu Y, Law CW, Shi W, et al. limma powers differential expression analyses for RNA-sequencing and microarray studies. *Nucleic Acids Res*. 2015;43:e47.
18. Phipson B, Lee S, Majewski IJ, Alexander WS, Smyth GK. Robust hyperparameter estimation protects against hypervariable genes and improves power to detect differential expression. *Ann Appl Stat*. 2016;10:946–63.
19. ComplexHeatmap R package. <https://academic.oup.com/bioinformatics/article/32/18/2847/1743594>.
20. Hickman SE, Kingery ND, Ohsumi TK, Borowsky ML, Wang L, Means TK, et al. The microglial sensome revealed by direct RNA sequencing. *Nat Neurosci*. 2013;16:1896–905.
21. Holtman IR, Raj DD, Miller JA, Schaafsma W, Yin Z, Brouwer N, et al. Induction of a common microglia gene expression signature by aging and neurodegenerative conditions: a co-expression meta-analysis. *Acta Neuropathol Commun*. 2015;3:31.

## Publisher's Note

Springer Nature remains neutral with regard to jurisdictional claims in published maps and institutional affiliations.